DTU Library

Entanglement-Enabled Advantage for Learning a Bosonic Random Displacement Channel

Oh, Changhun; Chen, Senrui; Wong, Yat; Zhou, Sisi; Huang, Hsin Yuan; Nielsen, Jens A.H.; Liu, Zheng Hao; Neergaard-Nielsen, Jonas S.; Andersen, Ulrik L.; Jiang, Liang

Total number of authors:
11

Published in:
Physical Review Letters

Link to article, DOI:
10.1103/PhysRevLett.133.230604

Publication date:
2024

Document Version
Publisher's PDF, also known as Version of record

Entanglement-Enabled Advantage for Learning a Bosonic Random Displacement Channel

Changhun Oh,[1,2,*] Senrui Chen,[1,*] Yat Wong,[1] Sisi Zhou,[3,4,5] Hsin-Yuan Huang,[4,6,7] Jens A. H. Nielsen,[8] Zheng-Hao Liu,[8] Jonas S. Neergaard-Nielsen,[8] Ulrik L. Andersen,[8] Liang Jiang,[1,†] and John Preskill[4,‡]

[1]*Pritzker School of Molecular Engineering, The University of Chicago, Chicago, Illinois 60637, USA*
[2]*Department of Physics, Korea Advanced Institute of Science and Technology, Daejeon 34141, Korea*
[3]*Perimeter Institute for Theoretical Physics, Waterloo, Ontario N2L 2Y5, Canada*
[4]*Institute for Quantum Information and Matter, California Institute of Technology, Pasadena, California 91125, USA*
[5]*Department of Physics and Astronomy and Institute for Quantum Computing, University of Waterloo, Ontario N2L 2Y5, Canada*
[6]*Center for Theoretical Physics, Massachusetts Institute of Technology, Cambridge, Massachusetts 02139, USA*
[7]*Google Quantum AI, Venice, California, USA*
[8]*Center for Macroscopic Quantum States (bigQ), Department of Physics, Technical University of Denmark, Building 307, Fysikvej, 2800 Kgs. Lyngby, Denmark*

(Received 19 February 2024; revised 27 August 2024; accepted 29 October 2024; published 6 December 2024)

We show that quantum entanglement can provide an exponential advantage in learning properties of a bosonic continuous-variable (CV) system. The task we consider is estimating a probabilistic mixture of displacement operators acting on n bosonic modes, called a random displacement channel. We prove that if the n modes are not entangled with an ancillary quantum memory, then the channel must be sampled a number of times exponential in n in order to estimate its characteristic function to reasonable precision; this lower bound on sample complexity applies even if the channel inputs and measurements performed on channel outputs are chosen adaptively or have unrestricted energy. On the other hand, we present a simple entanglement-assisted scheme that only requires a number of samples independent of n in the large squeezing and noiseless limit. This establishes an exponential separation in sample complexity. We then analyze the effect of photon loss and show that the entanglement-assisted scheme is still significantly more efficient than any lossless entanglement-free scheme under mild experimental conditions. Our work illuminates the role of entanglement in learning CV systems and points toward experimentally feasible demonstrations of provable entanglement-enabled advantage using CV quantum platforms.

DOI: 10.1103/PhysRevLett.133.230604

Quantum science and technology hold promise to revolutionize how we understand and interact with nature, enabling computational speedups [1], classically impossible communication tasks [2,3], and measurements with unprecedented sensitivity [4–6]. Rapid progress during the noisy intermediate-scale quantum era [7] has brought these promises closer to reality, but the challenge remains to demonstrate a rigorous quantum advantage for practical problems.

Over the past few years, there has been ongoing theoretical and experimental progress in exploring quantum computational advantage [8–16]. Another recent line of research seeks quantum advantage in learning [17–24], revealing that access to quantum memory enables us to learn properties of nature more efficiently. Specifically, Refs. [18,19] establish a framework for proving exponential separation in sample complexity between learning with and without a coherently controllable quantum memory. In contrast to its computational counterpart, this entanglement-enabled advantage in learning can be proven without invoking computational assumptions and can sometimes be more experimentally accessible. A proof-of-principle experiment has been conducted on Google's superconducting quantum processor using 40 qubits [18].

Most learning tasks studied so far are restricted to discrete-variable (DV) systems. It is natural to ask whether entanglement-enabled advantage can also be realized for learning properties of bosonic continuous-variable (CV) systems. This is particularly important because CV systems are ubiquitous in nature and have many applications in quantum information science, such as quantum sensing [6,8,25–27]. However, generalizing the results in DV systems to CV systems is challenging because bosonic systems have infinite-dimensional Hilbert spaces, complicating rigorous complexity analysis of learning. Recent progress has been achieved in studies of entanglement-enhanced learning of CV-state characteristic functions [28]; however, the lower

*These authors contributed equally to this letter.
†Contact author: liang.jiang@uchicago.edu
‡Contact author: preskill@caltech.edu

bounds obtained so far apply to a restricted class of learning strategies rather than to general entanglement-free schemes. There have also been recent works studying applications of statistical learning theory to CV systems [29–31].

Characterizing displacements applied to CV systems has many applications, including force sensing [32], dark matter search [33–35], gravitational wave detection [36], and Raman scattering spectroscopy [37]; therefore this task has drawn substantial recent attention [38,39]. In this Letter, we rigorously establish an entanglement-enabled advantage in learning a probabilistic mixture of n-mode displacement operations, called a "random displacement channel." Specifically, we prove that any schemes without ancillary quantum memory (i.e., entanglement-free) require exponentially many samples in n to learn the channel's characteristic function with good precision and high success probability. In contrast, we present a simple scheme utilizing entanglement with ancillary quantum memory (i.e., entanglement-assisted) that can achieve the same learning task with sample complexity independent of n, given access to two-mode squeezed vacuum (TMSV) states with sufficiently large squeezing parameter and Bell measurements (BMs). This establishes an exponential separation between learning with and without entanglement in the bosonic system (see Fig. 1).

Notably, our entanglement-assisted scheme achieves an exponential advantage using only Gaussian input state preparation and measurements that are experimentally feasible. Furthermore, we demonstrate the robustness of the entanglement-enabled advantage under realistic experimental conditions by analyzing the effects of photon loss, phase noise, and crosstalk, the most common noise sources in optical platforms, suggesting that for squeezing parameters and noise rates achievable in a state-of-the-art experiment, the advantage remains significant and thus can be realized shortly.

For DV systems, existing techniques for proving quantum advantages in learning typically involve characterizing the hardness of distinguishing a given state or channel from the maximally mixed state or completely depolarizing channel [17–19,23]. These states and channels are

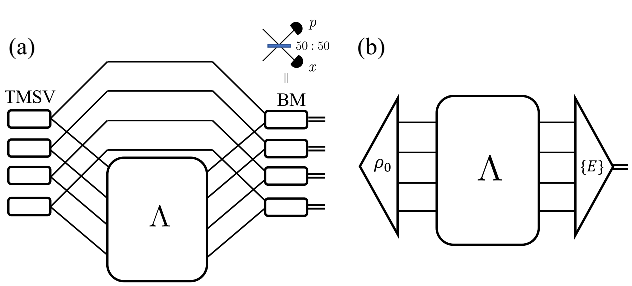

FIG. 1. Schemes for learning an n-mode random displacement channel Λ. (a) TMSV + BM, a specific entanglement-assisted (EA) scheme. (b) General entanglement-free (EF) scheme. See main text for more details.

ill-defined for CV systems; therefore we needed a different approach to establish an entanglement-enabled advantage without making reference to unphysical states (see the proof of Theorem 2). Another distinctive feature of our results is that our entanglement-free lower bound (Theorem 2) holds even for schemes that use input states with arbitrarily high energy (i.e., occupying an arbitrarily large Hilbert space), while the entanglement-assisted upper bound (Theorem 1) only uses finite energy input states.

Problem setup—We consider the task of learning an n-mode random displacement channel characterized by a probability distribution $p(\alpha)$ with $\alpha \in \mathbb{C}^n$, which transforms an input state $\hat{\rho}$ as

$$\Lambda(\hat{\rho}) = \int d^{2n}\alpha\, p(\alpha)\hat{D}(\alpha)\hat{\rho}\hat{D}^{\dagger}(\alpha), \tag{1}$$

where $\hat{D}(\alpha) := \otimes_{i=1}^{n} \hat{D}(\alpha_i)$ and $\hat{D}(\alpha_i) := \exp(\alpha_i \hat{a}_i^{\dagger} - \alpha_i^{*}\hat{a}_i)$ is the displacement operator for the ith mode. It can be equivalently described by the characteristic function of $p(\alpha)$, i.e., its Fourier transform, as [see Supplemental Material (SM), Sec. S1 [40] for the derivation]

$$\Lambda(\hat{\rho}) = \frac{1}{\pi^n}\int d^{2n}\beta\, \lambda(\beta)\mathrm{Tr}[\hat{\rho}\,\hat{D}(\beta)]\hat{D}^{\dagger}(\beta), \tag{2}$$

$$\lambda(\beta) := \int d^{2n}\alpha\, p(\alpha)e^{\alpha^{\dagger}\beta - \beta^{\dagger}\alpha}. \tag{3}$$

Here, because of the Fourier relation, $\lambda(\beta)$ with a large β contributes to rapidly oscillating $p(\alpha)$. Since the domain of β is infinite, we will focus on a restricted finite domain specified later. The goal is to learn the channel by estimating the characteristic function $\lambda(\beta)$; this is distinct from identifying a particular displacement drawn from the distribution $p(\alpha)$. The value of β of $\lambda(\beta)$ to be estimated is revealed only after all measurements are completed.

We focus on the separation between two types of learning schemes for the random displacement channel distinguished by whether the scheme uses entanglement between the system and an ancilla (see Fig. 1). Throughout this Letter, we define an entanglement-free scheme as being both ancilla-free and concatenation-free, i.e., the channel's output is measured destructively after each channel use. However, it is allowed to be adaptive; for each channel use, the input to the channel and the measurement may depend on measurement outcomes obtained in earlier rounds. This scenario is similar to Refs. [17,22]. Several recent works have obtained lower bounds on learning DV channels that hold even with concatenation [23,47,48], but for simplicity, we focus on concatenation-free schemes.

Schemes—Now, we present an entanglement-assisted scheme (see Fig. 1) inspired by the Pauli channel learning proposed in Ref. [23]. Consider an n-mode random displacement channel Λ_B acting on the n-mode system

B. To learn this channel, we prepare n CV Bell states with a finite squeezing parameter r, i.e., TMSV states, and half of the states go through the channel while the other half stays in quantum memory. Finally, we measure the output state by CV BMs, implemented by passing through 50∶50 beam splitters and performing homodyne measurement on output ports along different quadratures [27]. Formally, the BM positive operator-valued measure element labeled by $\{\zeta \in \mathbb{C}^n\}$ has the following form: $[I \otimes \hat{D}(\zeta)]|\Psi\rangle\langle\Psi|[I \otimes \hat{D}^\dagger(\zeta)]/\pi^n$; here, $|\Psi\rangle$ denotes the tensor product of n infinitely squeezed TMSV states, each proportional to $\sum_{k=0}^{\infty}|k\rangle|k\rangle$ when expressed in the Fock basis. To see how to learn a random displacement channel using this TMSV + BM scheme, we invoke the probability of obtaining outcome ζ from BM (see SM, Sec. S2A [40] for the derivation),

$$p_{EA}(\zeta) = \frac{1}{\pi^{2n}} \int d^{2n}\alpha\, \lambda(\alpha) e^{-e^{-2r}|\alpha|^2} e^{\alpha^\dagger\zeta - \zeta^\dagger\alpha}. \quad (4)$$

Fourier transforming to invert this relation, we obtain

$$\lambda(\beta) = e^{e^{-2r}|\beta|^2} \int d^{2n}\zeta\, p_{EA}(\zeta) e^{\zeta^\dagger\beta - \beta^\dagger\zeta} \coloneqq e^{e^{-2r}|\beta|^2}\lambda_{EA}(\beta). \quad (5)$$

This expression indicates that given N outcomes $\{\zeta^{(i)}\}_{i=1}^N$ from the TMSV + BM scheme, $\tilde{\lambda}(\beta) \coloneqq (1/N)e^{e^{-2r}|\beta|^2} \times \sum_{i=1}^N e^{\zeta^{(i)\dagger}\beta - \beta^\dagger\zeta^{(i)}}$ is an unbiased estimator of $\lambda(\beta)$. Note that the same set of samples can be used to estimate $\lambda(\beta)$ for different values of β just by modifying the estimator. Using the Hoeffding's bound, we prove the following theorem (see SM, Sec. S2A for the proof).

Theorem 1—For any n-mode random displacement channel Λ, after the TMSV + BM scheme with squeezing parameter r has learned from N copies of Λ, and then received a query $\beta \in \mathbb{C}^n$, it can provide an estimator $\tilde{\lambda}(\beta)$ of Λ's characteristic function $\lambda(\beta)$ such that $|\tilde{\lambda}(\beta) - \lambda(\beta)| \le \epsilon$ with probability at least $1-\delta$, with the number of samples $N = 8e^{2e^{-2r}|\beta|^2}\epsilon^{-2}\log 4\delta^{-1}$.

In Theorem 2 below we formulate a lower bound on the sample complexity for general entanglement-free schemes. First, though, let us compare the entanglement-assisted TMSV + BM scheme with a particular entanglement-free scheme that uses the vacuum state as input and heterodyne detection (Vacuum + Heterodyne). Here, heterodyne detection is defined as a projection onto the (overcomplete) basis of coherent states, i.e., $|\zeta\rangle\langle\zeta|/\pi^n$ with $\zeta \in \mathbb{C}^n$. This specific scheme helps us to understand the limitations of more general entanglement-free schemes that are captured more fully by Theorem 2.

In this scheme, the probability of obtaining the outcome ζ is (see SM, Sec. S2B [40])

$$p_{\rm VH}(\zeta) = \frac{1}{\pi^{2n}} \int d^{2n}\alpha\, \lambda(\alpha) e^{\alpha^\dagger\zeta - \zeta^\dagger\alpha} e^{-|\alpha|^2}. \quad (6)$$

In fact, the Vacuum + Heterodyne scheme can be understood as the TMSV + BM scheme with $r = 0$. Inverting this relation by Fourier transforming, we again express the channel's characteristic function by the measurement probability distribution

$$\lambda(\beta) = e^{|\beta|^2} \int d^{2n}\zeta\, p_{\rm VH}(\zeta) e^{\zeta^\dagger\beta - \beta^\dagger\zeta} \coloneqq e^{|\beta|^2}\lambda_{\rm VH}(\beta), \quad (7)$$

which yields another unbiased estimator $\tilde{\lambda}(\beta) \coloneqq (1/N)e^{|\beta|^2} \times \sum_{i=1}^N e^{\zeta^{(i)\dagger}\beta - \beta^\dagger\zeta^{(i)}}$ given N outcomes $\{\zeta^{(i)}\}_{i=1}^N$. Comparing to (5), the r-dependent prefactor is missing from (7). Specifically, if we confine β to $|\beta|^2 \le \kappa n$ with a constant $\kappa > 0$, we obtain upper bounds on the sample complexity for achieving an error ϵ with success probability $1-\delta$ using each scheme,

$$N_{\rm EA} = O(e^{2e^{-2r}\kappa n}\epsilon^{-2}\log\delta^{-1}),$$
$$N_{\rm VH} = O(e^{2\kappa n}\epsilon^{-2}\log\delta^{-1}). \quad (8)$$

In particular, if we choose $r = \Omega(\log n)$, the sample complexity of the entanglement-assisted scheme becomes independent of the number of modes n, while our upper bound on that of the entanglement-free scheme increases exponentially with n. Since the accessible squeezing parameter is bounded in practice, though, we will consider the sample complexities for constant r below.

To illustrate the difference, we compare the two strategies with a single-mode example, characterized by

$$p(\alpha) = \frac{2\sigma^2}{\pi} e^{-2\sigma^2|\alpha|^2}[\cos^2(\alpha_r\gamma_i - \alpha_i\gamma_r) + \sin^2(\alpha_r\gamma_r + \alpha_i\gamma_i)], \quad (9)$$

$$\lambda(\beta) = e^{-\frac{|\beta|^2}{2\sigma^2}} + \frac{1}{4}e^{-\frac{|\beta-\gamma|^2}{2\sigma^2}} + \frac{1}{4}e^{-\frac{|\beta+\gamma|^2}{2\sigma^2}} - \frac{1}{4}e^{-\frac{|\beta-i\gamma|^2}{2\sigma^2}} - \frac{1}{4}e^{-\frac{|\beta+i\gamma|^2}{2\sigma^2}}, \quad (10)$$

with $\sigma = 0.3$, $\gamma_r = 1.6$, $\gamma_i = 0$ ($\gamma \coloneqq \gamma_r + i\gamma_i$), and $r = 2$ for the TMSV + BM scheme. Figure 2, presenting the underlying output probability distributions and their characteristic functions from Eqs. (4)–(7), clearly shows that in the TMSV + BM scheme with a sufficient squeezing parameter, the resultant probability distribution and characteristic function are almost identical to the ideal case. However, for the Vacuum + Heterodyne scheme, the vacuum noise distorts the initial probability distribution so significantly that we cannot see the signal clearly, making it harder to estimate the original characteristic function.

Lower bound—Our upper bound on the sample complexity of the Vacuum + Heterodyne scheme scales exponentially with n. Can this scaling be improved using more advanced entanglement-free schemes, such as general-dyne

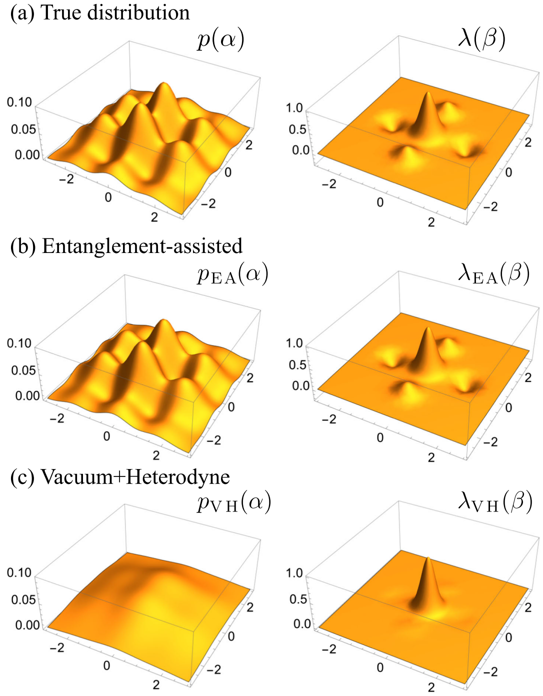

FIG. 2. Comparison between (a) the true distribution, (b) TMSV + BM, and (c) Vacuum + Heterodyne strategies. The left panel represents the true probability distribution or the measurement outcome probability distribution for each scheme [Eqs. (4), (6)]. The right panel represents the characteristic function of the corresponding distributions [Eqs. (5), (7)].

detection or photon-number resolving measurements [49], or by non-Gaussian resources like Gottesman-Kitaev-Preskill states [50]? Here, using information-theoretic methods, we prove an exponential sample complexity lower bound for any entanglement-free scheme. This highlights the indispensable role of entanglement for efficiently learning random displacement channels. Our result is as follows.

Theorem 2—Let Λ be an arbitrary n-mode random displacement channel ($n \geq 8$) and consider an entanglement-free scheme that uses N copies of Λ. After all measurements are completed, the scheme receives the query $\beta \in \mathbb{C}^n$ and returns an estimate $\tilde{\lambda}(\beta)$ of Λ's characteristic function $\lambda(\beta)$. Suppose that, with success probability at least $2/3$, $|\tilde{\lambda}(\beta) - \lambda(\beta)| \leq \epsilon \leq 0.24$ for all β such that $|\beta|^2 \leq n\kappa$ and all Λ. Then $N \geq 0.01\epsilon^{-2}(1 + 1.98\kappa)^n$.

Here, the choice of success probability $2/3$ is arbitrary and can be easily amplified. Comparing with the entanglement-assisted sample complexity given in Eq. (8), Theorem 2 establishes a separation exponential in n for cutoff coefficient $\kappa = O(1)$ and squeezing parameter $r = \Omega(\log n)$. The intuition underlying this theorem is that displacement operators do not generally commute with each other. Consequently, entanglement-free measurements can resolve $\lambda(\beta)$ for only a small portion of β space. We sketch the proof below and leave the full details to SM, Sec. S3 [40].

Proof sketch—We begin by defining the following family of "3-peak" random displacement channels, $\Lambda^{\epsilon,\sigma}_{\text{3-peak}} = \{\Lambda_\gamma\}_{\gamma \in \mathbb{C}^n}$, whose characteristic functions and distributions of displacement are, respectively,

$$\lambda_\gamma(\beta) = e^{-\frac{|\beta|^2}{2\sigma^2}} + 2i\epsilon_0 e^{-\frac{|\beta-\gamma|^2}{2\sigma^2}} - 2i\epsilon_0 e^{-\frac{|\beta+\gamma|^2}{2\sigma^2}}, \tag{11}$$

$$p_\gamma(\alpha) \propto e^{-2\sigma^2|\alpha|^2}\{1 + 4\epsilon_0 \sin[2(\gamma_i\alpha_r - \gamma_r\alpha_i)]\}. \tag{12}$$

with positive parameters σ and $\epsilon \coloneqq 0.98\epsilon_0$. Note that the channel with $\sigma \to 0$ and $\gamma = 0$ resembles the completely depolarizing channel used in Refs. [18,23], which outputs the maximally mixed state in the infinite-dimensional Hilbert space, $\propto \sum_{k=0}^{\infty} |k\rangle\langle k|$, that is mathematically ill-defined and thus unphysical; however, because σ is strictly larger than zero throughout the proof, the channels are well-defined. We will show that, even with the prior knowledge that the channel is from this family, it is still hard for entanglement-free schemes to achieve the learning tasks.

The key idea is to reduce learning to hypothesis testing. Consider the following game between Alice and Bob. Alice chooses one of two hypotheses with equal probability: (1) Set $\Lambda = \Lambda_0$; (2) Set $\Lambda = \Lambda_\gamma$ for γ sampled from a Gaussian distribution whose variance is determined by κ. Next, Alice allows Bob to use the channel Λ N times, and Bob uses any entanglement-free schemes to learn from these channel uses. After Bob has finished all quantum measurements and keeps only classical data, Alice reveals some auxiliary information to Bob, and Bob then decides whether Alice has chosen (1) or (2).

Using a learning scheme satisfying the assumptions of Theorem 2, Bob can guess correctly with high probability; Thus, the outcome distributions of Bob's scheme under hypotheses (1) and (2) must have a large total variation distance (TVD). Meanwhile, we prove that the contribution from each use of Λ to the TVD is exponentially small using a new technique inspired by Ref. [51], which derived the maximum fidelity of Gaussian random displacement channels. Therefore, the number of channel uses N must be exponentially large to ensure a large TVD, which gives us the desired lower bound on the sample complexity. ■

Effect of noise—Now, for practical applications, we analyze the effect of dominant noise sources in optical platforms on the entanglement-assisted scheme and demonstrate its robustness against them, implying that the advantage is realizable shortly. We discuss the photon-loss effect in the main text, while phase diffusion and measurement crosstalk are covered in SM, Secs. S2D and E. Photon loss transforms the relevant bosonic operator $\hat{a}$ to $\sqrt{T}\hat{a} + \sqrt{1-T}\hat{e}$, where T is the transmission rate and $\hat{e}$ is the environmental mode, i.e., $1 - T$ is the loss rate. We consider two different places where the loss occurs: one is

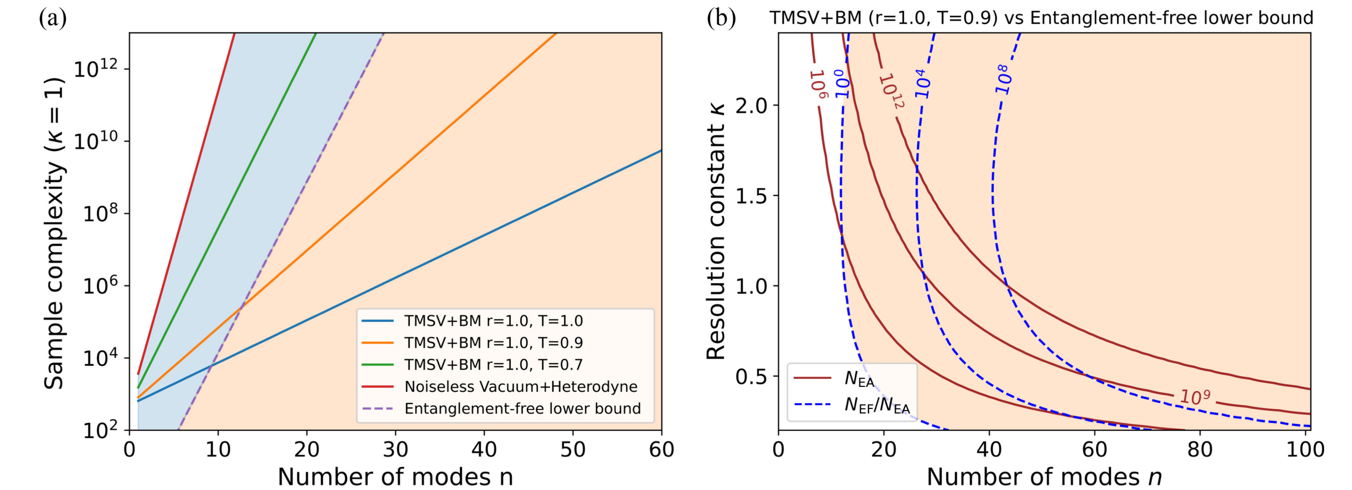

FIG. 3. (a) Comparison of TMSV + BM (with different loss rates), Vacuum + Heterodyne, and the entanglement-free lower bound at $\kappa = 1$. The task is to estimate any $\lambda(\beta)$ such that $|\beta|^2 \leq \kappa n$ with precision $\varepsilon = 0.2$ and success probability $1 - \delta = 2/3$. The orange region represents a rigorous advantage over all entanglement-free schemes. The blue region represents an advantage over noiseless Vacuum + Heterodyne. (b) Comparison of the TMSV + BM scheme with squeezing parameter $r = 1.0$ and loss rate $1 - T = 0.1$ with the entanglement-free lower bound of Theorem 2. (See SM, Sec. S3A, for further practical considerations.) The task is the same as (a). The brown solid contour lines represent the sample complexity of TMSV + BM given by Theorem 3. The blue dashed contour lines represent the ratio of sample complexity between the entanglement-free lower bound and TMSV + BM, indicating the entanglement-enabled advantage.

before applying the channel with loss rate $1 - T_b$ to model the preparation imperfection, and the other is after applying the channel and before the perfect BM with loss rate $1 - T_a$, which models an imperfect BM [27]. As before, we derive the relation between the measurement probability distribution and the characteristic function of the channel (with appropriate rescaling of the phase),

$$\lambda(\beta) = e^{e^{-2r_{\text{eff}}}|\beta|^2} \int d^{2n}\zeta\, p_{\text{loss}}(\zeta) e^{(\zeta^\dagger \beta - \beta^\dagger \zeta)/\sqrt{T_a}}, \tag{13}$$

where we define an effective squeezing parameter

$$r_{\text{eff}} \coloneqq -\frac{1}{2}\log\left(T_b e^{-2r} + (1 - T_b) + \frac{1 - T_a}{T_a}\right), \tag{14}$$

which incorporates the loss rates. Because loss degrades the advantage from squeezing, the upper bound on sample complexity in Theorem 1 is modified as follows (see SM, Sec. S2C, for the proof).

Theorem 3—For the same task as in Theorem 1, a TMSV + BM scheme with squeezing parameter r and transmission rates before and after the channel T_b and T_a respectively, can estimate any $\lambda(\beta)$ to error ϵ with success probability $1 - \delta$ using the number of samples $N = 8e^{2e^{-2r_{\text{eff}}}|\beta|^2}\epsilon^{-2}\log 4\delta^{-1}$, where r_{eff} is defined according to Eq. (14).

Thus, when $|\beta|^2 \leq \kappa n$ with a constant $\kappa > 0$, $T_b = 1 - O(1/n)$, $T_a = 1 - O(1/n)$, and $r = \Omega(\log n)$, the sample complexity becomes $N = O(\epsilon^{-2}\log\delta^{-1})$ as in the lossless case. For practically relevant squeezing and including loss prior to BM, we compare the sample complexity for the lossy TMSV + BM protocol and the lossless entanglement-free lower bound in Fig. 3, finding a significant entanglement-enabled advantage in realistic experimental settings. Specifically, for reasonable parameter choices such as squeezing parameter $r = 1$, loss rate 10%, and $\kappa = O(1)$, we can achieve a factor of 10^4 (10^8) advantage for around $n = 30$ (60) modes. Although the 10^9 number of samples required to achieve the advantage seems large, the state-of-the-art quantum optics experiments (e.g., Refs. [52,53]) can attain such number of samples in a reasonable time with high sampling rate up to 160 GHz.

Discussion—We proved that schemes exploiting entanglement with an ancillary quantum memory can learn n-mode random displacement channels with exponentially fewer samples compared to entanglement-free schemes. Our proof technique generalizes the information-theoretic framework for learning studied in DV quantum systems [17,19] to the CV setting. We anticipate that many other results concerning DV systems can be generalized using similar methods to CV learning tasks, such as learning CV quantum states or other CV channels. Also, our analysis suggests that the separation in sample complexity between entanglement-assisted and entanglement-free protocols may soon be realized experimentally.

Besides their theoretical interest, random displacement channels can be practically relevant in, e.g., modeling noise in bosonic systems. As in qubit cases [54], we expect that noise tailoring methods can transform more general noise models into random displacement channels; therefore efficiently learning random displacement channels can be useful for benchmarking CV quantum systems [39,55,56] and error mitigation.

Displacement estimation is also studied in quantum metrology (see, e.g., [57–59]). A task often considered in metrology is learning an unknown *unitary* displacement or phase transformation acting independently on each mode [52,58,60–63], whereas the task analyzed in this Letter is learning an unknown *mixture* of multimode displacements. Furthermore, while the goal in metrology is typically to learn one or a few parameters, in our case, the parameter space is very large. Therefore, the methodology in the two settings is quite different. Connections between metrology and bosonic channel learning are worthy of further exploration.

Acknowledgments—We thank Mankei Tsang, Yuxin Wang, Ronald de Wolf, Mingxing Yao, and Ming Yuan for insightful discussions. C. O., S. C., Y. W., and L. J. acknowledge support from the ARO (W911NF-23-1-0077), ARO MURI (W911NF-21-1-0325), AFOSR MURI (FA9550-19-1-0399, FA9550-21-1-0209), NSF (OMA-1936118, ERC-1941583, OMA-2137642), NTT Research, Packard Foundation (2020-71479). J. P. acknowledges support from the U.S. Department of Energy Office of Science, Office of Advanced Scientific Computing Research (DE-NA0003525, DE-SC0020290), the U.S. Department of Energy, Office of Science, National Quantum Information Science Research Centers, Quantum Systems Accelerator, and the National Science Foundation (PHY-1733907). The Institute for Quantum Information and Matter is an NSF Physics Frontiers Center. S. Z. acknowledges funding provided by the Institute for Quantum Information and Matter and Perimeter Institute for Theoretical Physics, a research institute supported in part by the Government of Canada through the Department of Innovation, Science and Economic Development Canada and by the Province of Ontario through the Ministry of Colleges and Universities. J. A. H. N., Z.-H. L., J. S. N.-N., and U. L. A acknowledge support from DNRF (bigQ, DNRF142), IFD (PhotoQ, 1063-00046A), EU (CLUSTEC, ClusterQ ERC-101055224, GTGBS MC-416 101106833) and NNF (CBQS, 24SA0088433). C. O. acknowledges support from Quantum Technology R&D Leading Program (Quantum Computing) (RS-2024-00431768) through the National Research Foundation of Korea (NRF) funded by the Korean government [Ministry of Science and ICT (MSIT)].

[1] M. A. Nielsen and I. Chuang, *Quantum Computation and Quantum Information* (Cambridge University Press, Cambridge, England, 2002).
[2] N. Gisin and R. Thew, Quantum communication, Nat. Photonics **1**, 165 (2007).
[3] H. J. Kimble, The quantum internet, Nature (London) **453**, 1023 (2008).
[4] V. Giovannetti, S. Lloyd, and L. Maccone, Quantum metrology, Phys. Rev. Lett. **96**, 010401 (2006).
[5] V. Giovannetti, S. Lloyd, and L. Maccone, Advances in quantum metrology, Nat. Photonics **5**, 222 (2011).
[6] E. Polino, M. Valeri, N. Spagnolo, and F. Sciarrino, Photonic quantum metrology, AVS Quantum Sci. **2**, 024703 (2020).
[7] J. Preskill, Quantum computing in the NISQ era and beyond, Quantum **2**, 79 (2018).
[8] S. Aaronson and A. Arkhipov, The computational complexity of linear optics, in *Proceedings of the 43rd Annual ACM Symposium on Theory of Computing* (ACM, New York, 2011), pp. 333–342.
[9] S. Boixo, S. V. Isakov, V. N. Smelyanskiy, R. Babbush, N. Ding, Z. Jiang, M. J. Bremner, J. M. Martinis, and H. Neven, Characterizing quantum supremacy in near-term devices, Nat. Phys. **14**, 595 (2018).
[10] F. Arute, K. Arya, R. Babbush, D. Bacon, J. C. Bardin, R. Barends, R. Biswas, S. Boixo, F. G. Brandao, D. A. Buell *et al.*, Quantum supremacy using a programmable superconducting processor, Nature (London) **574**, 505 (2019).
[11] Y. Wu, W.-S. Bao, S. Cao, F. Chen, M.-C. Chen, X. Chen, T.-H. Chung, H. Deng, Y. Du, D. Fan *et al.*, Strong quantum computational advantage using a superconducting quantum processor, Phys. Rev. Lett. **127**, 180501 (2021).
[12] H.-S. Zhong, H. Wang, Y.-H. Deng, M.-C. Chen, L.-C. Peng, Y.-H. Luo, J. Qin, D. Wu, X. Ding, Y. Hu *et al.*, Quantum computational advantage using photons, Science **370**, 1460 (2020).
[13] H.-S. Zhong, Y.-H. Deng, J. Qin, H. Wang, M.-C. Chen, L.-C. Peng, Y.-H. Luo, D. Wu, S.-Q. Gong, H. Su *et al.*, Phase-programmable Gaussian boson sampling using stimulated squeezed light, Phys. Rev. Lett. **127**, 180502 (2021).
[14] L. S. Madsen, F. Laudenbach, M. F. Askarani, F. Rortais, T. Vincent, J. F. Bulmer, F. M. Miatto, L. Neuhaus, L. G. Helt, M. J. Collins *et al.*, Quantum computational advantage with a programmable photonic processor, Nature (London) **606**, 75 (2022).
[15] A. Morvan, B. Villalonga, X. Mi, S. Mandra, A. Bengtsson, P. Klimov, Z. Chen, S. Hong, C. Erickson, I. Drozdov *et al.*, Phase transition in random circuit sampling, arXiv:2304.11119.
[16] Y.-H. Deng *et al.*, Gaussian boson sampling with pseudo-photon-number-resolving detectors and quantum computational advantage, Phys. Rev. Lett. **131**, 150601 (2023).
[17] H.-Y. Huang, R. Kueng, and J. Preskill, Information-theoretic bounds on quantum advantage in machine learning, Phys. Rev. Lett. **126**, 190505 (2021).
[18] H.-Y. Huang, M. Broughton, J. Cotler, S. Chen, J. Li, M. Mohseni, H. Neven, R. Babbush, R. Kueng, J. Preskill, and J. R. McClean, Quantum advantage in learning from experiments, Science **376**, 1182 (2022).
[19] S. Chen, J. Cotler, H.-Y. Huang, and J. Li, Exponential separations between learning with and without quantum memory, in *Proceedings of the 2021 IEEE 62nd Annual Symposium on Foundations of Computer Science (FOCS)* (IEEE, New York, 2022), pp. 574–585.
[20] M. C. Caro, Learning quantum processes and Hamiltonians via the Pauli transfer matrix, arXiv:2212.04471.

[21] S. Bubeck, S. Chen, and J. Li, Entanglement is necessary for optimal quantum property testing, in *Proceedings of the 2020 IEEE 61st Annual Symposium on Foundations of Computer Science (FOCS)* (IEEE, New York, 2020), pp. 692–703.

[22] D. Aharonov, J. Cotler, and X.-L. Qi, Quantum algorithmic measurement, Nat. Commun. **13**, 887 (2022).

[23] S. Chen, S. Zhou, A. Seif, and L. Jiang, Quantum advantages for Pauli channel estimation, Phys. Rev. A **105**, 032435 (2022).

[24] Z. M. Rossi, J. Yu, I. L. Chuang, and S. Sugiura, Quantum advantage for noisy channel discrimination, Phys. Rev. A **105**, 032401 (2022).

[25] S. L. Braunstein and P. Van Loock, Quantum information with continuous variables, Rev. Mod. Phys. **77**, 513 (2005).

[26] C. Weedbrook, S. Pirandola, R. García-Patrón, N. J. Cerf, T. C. Ralph, J. H. Shapiro, and S. Lloyd, Gaussian quantum information, Rev. Mod. Phys. **84**, 621 (2012).

[27] A. Serafini, *Quantum Continuous Variables: A Primer of Theoretical Methods* (Taylor & Francis, Oxford, 2017).

[28] Y.-D. Wu, G. Chiribella, and N. Liu, Efficient learning of continuous-variable quantum states, Phys. Rev. Res. **6**, 033280 (2024).

[29] S. Becker, N. Datta, L. Lami, and C. Rouze, Classical shadow tomography for continuous variables quantum systems, IEEE Trans. Inf. Theory **70**, 3427 (2024).

[30] S. Gandhari, V. V. Albert, T. Gerrits, J. M. Taylor, and M. J. Gullans, Precision bounds on continuous-variable state tomography using classical shadows, PRX Quantum **5**, 010346 (2024).

[31] M. Rosati, A learning theory for quantum photonic processors and beyond, Quantum **8**, 1433 (2024).

[32] E. Gavartin, P. Verlot, and T. J. Kippenberg, A hybrid on-chip optomechanical transducer for ultrasensitive force measurements, Nat. Nanotechnol. **7**, 509 (2012).

[33] P. Sikivie, Experimental tests of the "invisible" axion, Phys. Rev. Lett. **51**, 1415 (1983).

[34] A. J. Brady, C. Gao, R. Harnik, Z. Liu, Z. Zhang, and Q. Zhuang, Entangled sensor-networks for dark-matter searches, PRX Quantum **3**, 030333 (2022).

[35] K. M. Backes, D. A. Palken, S. A. Kenany, B. M. Brubaker, S. Cahn, A. Droster, G. C. Hilton, S. Ghosh, H. Jackson, S. K. Lamoreaux *et al.*, A quantum enhanced search for dark matter axions, Nature (London) **590**, 238 (2021).

[36] D. Ganapathy, W. Jia, M. Nakano, V. Xu, N. Aritomi, T. Cullen, N. Kijbunchoo, S. Dwyer, A. Mullavey, L. McCuller *et al.*, Broadband quantum enhancement of the LIGO detectors with frequency-dependent squeezing, Phys. Rev. X **13**, 041021 (2023).

[37] R. B. de Andrade, H. Kerdoncuff, K. Berg-Sørensen, T. Gehring, M. Lassen, and U. L. Andersen, Quantum-enhanced continuous-wave stimulated raman scattering spectroscopy, Optica **7**, 470 (2020).

[38] J. W. Gardner, T. Gefen, S. A. Haine, J. J. Hope, J. Preskill, Y. Chen, and L. McCuller, Stochastic waveform estimation at the fundamental quantum limit, arXiv:2404.13867.

[39] C. H. Valahu, T. Navickas, M. J. Biercuk, and T. R. Tan, Benchmarking bosonic modes for quantum information with randomized displacements, arXiv:2405.15237.

[40] See Supplemental Material at http://link.aps.org/supplemental/10.1103/PhysRevLett.133.230604 for the derivation of output probability distributions of each scheme and the detailed proof of theorems, which includes Refs. [41–46].

[41] A. Ferraro, S. Olivares, and M. G. Paris, Gaussian states in continuous variable quantum information, arXiv:quant-ph/0503237.

[42] K. Kornelson and D. Larson, Rank-one decomposition of operators and construction of frames, Contemp. Math. **345**, 203 (2004).

[43] K. R. Castleman, *Digital Image Processing* (Prentice Hall Press, Englewood Cliffs, NJ, 1996).

[44] S. Barnett and P. M. Radmore, *Methods in Theoretical Quantum Optics* (Oxford University Press, New York, 2002), Vol. 15.

[45] X. Zhan, *Matrix Theory* (American Mathematical Society, Providence, 2013), Vol. 147.

[46] M. Ghosh, Exponential tail bounds for chisquared random variables, J. Stat. Theory Pract. **15**, 1 (2021).

[47] S. Chen and W. Gong, Futility and utility of a few ancillas for Pauli channel learning, arXiv:2309.14326.

[48] S. Chen, C. Oh, S. Zhou, H.-Y. Huang, and L. Jiang, Tight bounds on Pauli channel learning without entanglement, Phys. Rev. Lett. **132**, 180805 (2024).

[49] D. Schuster, A. A. Houck, J. Schreier, A. Wallraff, J. Gambetta, A. Blais, L. Frunzio, J. Majer, B. Johnson, M. Devoret *et al.*, Resolving photon number states in a superconducting circuit, Nature (London) **445**, 515 (2007).

[50] D. Gottesman, A. Kitaev, and J. Preskill, Encoding a qubit in an oscillator, Phys. Rev. A **64**, 012310 (2001).

[51] C. M. Caves and K. Wódkiewicz, Fidelity of gaussian channels, Open Syst. Inf. Dyn. **11**, 309 (2004).

[52] X. Guo, C. R. Breum, J. Borregaard, S. Izumi, M. V. Larsen, T. Gehring, M. Christandl, J. S. Neergaard-Nielsen, and U. L. Andersen, Distributed quantum sensing in a continuous-variable entangled network, Nat. Phys. **16**, 281 (2020).

[53] A. Inoue, T. Kashiwazaki, T. Yamashima, N. Takanashi, T. Kazama, K. Enbutsu, K. Watanabe, T. Umeki, M. Endo, and A. Furusawa, Toward a multi-core ultra-fast optical quantum processor: 43-Ghz bandwidth real-time amplitude measurement of 5-db squeezed light using modularized optical parametric amplifier with 5g technology, Appl. Phys. Lett. **122**, 104001 (2023).

[54] J. J. Wallman and J. Emerson, Noise tailoring for scalable quantum computation via randomized compiling, Phys. Rev. A **94**, 052325 (2016).

[55] Y.-D. Wu and B. C. Sanders, Efficient verification of bosonic quantum channels via benchmarking, New J. Phys. **21**, 073026 (2019).

[56] G. Bai and G. Chiribella, Test one to test many: A unified approach to quantum benchmarks, Phys. Rev. Lett. **120**, 150502 (2018).

[57] H. Shi and Q. Zhuang, Ultimate precision limit of noise sensing and dark matter search, npj Quantum Inf. **9**, 27 (2023).

[58] Q. Zhuang, Z. Zhang, and J. H. Shapiro, Distributed quantum sensing using continuous-variable multipartite entanglement, Phys. Rev. A **97**, 032329 (2018).

[59] Y. Xia, W. Li, W. Clark, D. Hart, Q. Zhuang, and Z. Zhang, Demonstration of a reconfigurable entangled radio-frequency photonic sensor network, Phys. Rev. Lett. **124**, 150502 (2020).

[60] K. Duivenvoorden, B. M. Terhal, and D. Weigand, Single-mode displacement sensor, Phys. Rev. A **95**, 012305 (2017).
[61] C. Oh, C. Lee, S. H. Lie, and H. Jeong, Optimal distributed quantum sensing using gaussian states, Phys. Rev. Res. **2**, 023030 (2020).
[62] C. Oh, L. Jiang, and C. Lee, Distributed quantum phase sensing for arbitrary positive and negative weights, Phys. Rev. Res. **4**, 023164 (2022).
[63] H. Kwon, Y. Lim, L. Jiang, H. Jeong, and C. Oh, Quantum metrological power of continuous-variable quantum networks, Phys. Rev. Lett. **128**, 180503 (2022).